SWELLING BEHAVIOUR AND PERMEABILITY OF COMPACTED BENTONITES AT HIGH SALINITY AS INFLUENCED BY FLUID PRESSURE CHANGES

Meleshyn A. Yu.

Gesellschaft für Anlagen und Reaktorsicherheit (GRS) gGmbH, Braunschweig, Germany

Article received on March 10, 2020

This study presents results of two series of permeameter experiments with 15 bentonites compacted to a bulk density of 1.6 g/cm^3 before and after one-year contact with a model clay porewater with a salinity of 155 g/l. For four original bentonites, a double-peak pattern of swelling pressure evolution was revealed, which was observed previously only at much lower salinities. For 80% of bentonites, swelling pressure and permeability were in the range of 0.8–4.8 MPa and $7{\cdot}10^{-20}$–$3{\cdot}10^{-18}$ m^2 (for original ones) as well as 0.5–2.2 MPa and $4{\cdot}10^{-19}$–$6{\cdot}10^{-18}$ m^2 (for ones after one-year contact). A fluid pressure surge of 12.6 MPa caused no hydraulic fracturing of original bentonites. This observation challenges the validity of threshold values of a few MPa for onset of hydraulic fracturing in compacted bentonites proposed earlier using an alternative experimental method. Yet, this fluid pressure surge and a moderate one of 0.3 MPa caused a decrease of swelling pressure by up to 66% – an effect, which need to be accounted for when designing and assessing the performance of bentonite-based barriers in a geological repository.

Keywords: *radioactive waste, bentonite, swelling pressure, permeability, fluid pressure, engineered barriers, geological repository*

Introduction

Swelling pressure and permeability of bentonite-based geotechnical barriers represent key parameters for development of sealing concepts of geological repositories of high-level radioactive waste in clay and crystalline formations, as geotechnical barriers must be designed to have a sufficiently low permeability in order to minimise radionuclide migration from repository and to achieve safe enclosure of radioactive waste [1, 2]. At the disposal depth of several hundred meters, these barriers will experience increase of fluid pressure by several megapascals in the course of establishing hydraulic conditions characteristic of the host formation after the repository closure. Besides, gas production and accumulation in repository may cause additional fluid pressure increases. In this relation, a concern was raised whether in response to such fluid pressure increases, a hydraulic fracturing of compacted bentonites may occur, which would be accompanied by formation of preferential water infiltration and radionuclide migration pathways through bentonite-based geotechnical barriers or along their interfaces with containers with radioactive waste, host rock or tunnel lining [3, 4].

The phenomenon of hydraulic fracturing is closely related to swelling behaviour and permeability characteristics of compacted bentonites, which itself depend on several parameters, one of which is the salinity of infiltrating solution. Clay formations in Northern Germany potentially capable to host

a geological repository are characterised with a high salinity [1]. Therefore, determination of swelling pressure and permeability for compacted bentonites before and after a prolonged contact with a model porewater was a main goal of the present study. Fluid pressure surges in the course of the experiments occurred as described below provided additional results that may be of relevance for estimation of the effect of fluid pressure increases on sealing performance of compacted bentonites in a geological repository.

Materials and Methods

Bentonites and solution

As model solution for clay porewaters of Lower Cretaceous clay considered as a potential host rock for a geological repository in Germany [1] was used a cap rock solution diluted to a salinity of 155 g/l (further in the text VGH, from German "verdünnte Gipshutlösung") and consisting of NaCl (145.9 g/l), $CaCl_2$ (3.5 g/l), Na_2SO_4 (5.4 g/l), and KCl (0.4 g/l). Bentonites B04 and SD80 (Greece, Milos), B09 (USA, Wyoming), B10, B11, and B12 (India, Kutch), B13 (Hungary), B16 (Germany, Bavaria), B19 (Spain, Almeria), B23 (Argentina), B31 (Armenia), B36 (Slovakia, Liskovec), B37 (Slovakia, Jelsovy Potok), B38 (Russia), and B49 (Turkey, Balekesir) with smectite content varying between 63 and 91 wt.% [5] were kindly provided by Dr. Stephan Kaufhold (BGR, Hannover). Bentonites were pre-crushed in a jaw crusher and ground with Planetary Ball Mill PM 400 (Retsch) for 30 min at 230 rpm using three large (3 cm) and two small (2 cm) balls in the grinding jar. Bentonite powders were dried at 50 °C before use in the first series of experiments. In the second series, bentonite powders were mixed with VGH at a solid-liquid ratio of 1:2 and kept in contact for 430 ± 11 days at 25 °C in glass vessels, welded after purging bentonite suspensions with N_2. After the contact and decantation of solutions, bentonites were air-dried and ground to powder before use.

Experimental set-up

Experiments were carried out using 12 (in the first series) and 20 (in the second series) constant-head, rigid-wall permeameter cells made of titan (10 cells) and stainless steel (10 cells) (Figure 1). Bentonite powder was filled in between the porous plates of a cell and, after installing the load-transfer ram and press flange above the top porous plate, statically compacted to a pellet with a diameter of 5 cm, a height of 1 cm, and a bulk density of 1.6 g/cm^3. The cap nut of the press flange was then tightened without adding axial stress. In the second series, a triple loading/unloading of bentonites was carried out additionally in advance of tightening the cap nut in order to study the effect of mechanical pre-treatment on the swelling pressure behaviour. Dry densities of compacted bentonites were calculated from the bulk density of 1.6 g/cm^3 and the water content. Water content of original bentonites was determined upon drying at 105 °C for 3 up to 7 days to equal in average 4.1 ± 1.8 mass % and varied between 0.6 mass % for B09 and 1.7 mass % for B31 up to 5.8 mass % for B37 and 8.5 mass % for B49. Accordingly, dry density of original compacted bentonites was in average 1.54 ± 0.03 g/cm^3 and varied between 1.47 g/cm^3 for B49 and 1.51 g/cm^3 for B37 up to 1.57 g/cm^3 for B31 and 1.59 g/cm^3 for B09.

Figure 1. A construction drawing of the permeameter cell (a); supply of VGH to inlets at cell bottoms from burettes (b) to saturate bentonites and by a valve pump (c) to measure the permeability (regard plastic vessels connected to outlets at cell tops to collect percolating solutions)

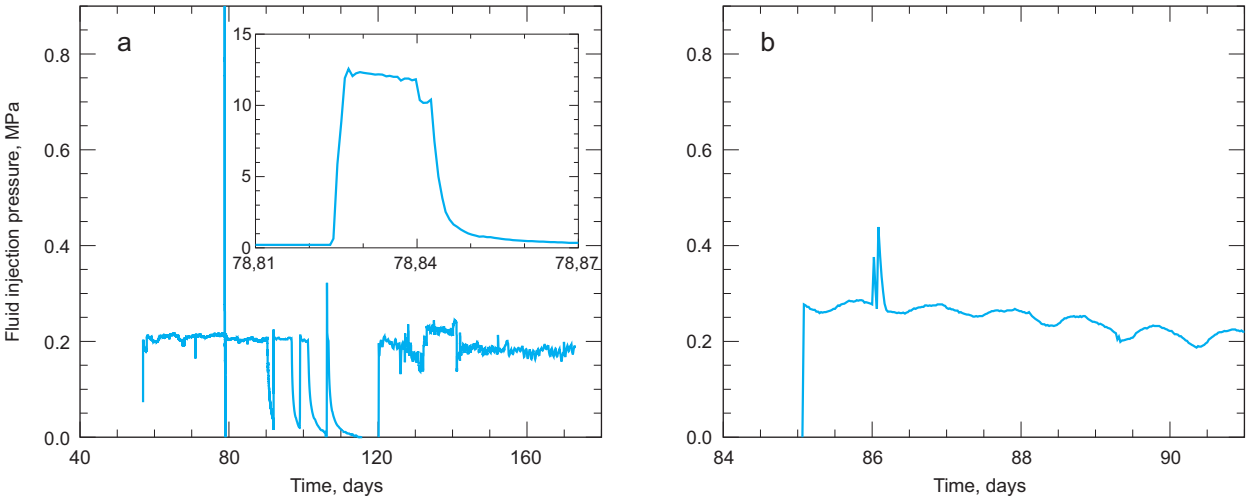

Figure 2..:Fluid injection pressure (MPa) in the first (a) and second (b) series. Inset shows a close-up of a fluid pressure surge

Compacted bentonites were allowed to saturate by absorbing VGH from a burette connected to an inlet at the cell bottom to let the trapped air to escape from an outlet at the cell top for up to five weeks, then to the inlet at the cell top for up to five weeks to reach as homogeneous saturation of bentonite as possible (Figure 1). Swelling of compacted bentonites upon saturation was assumed to seal off possible flow pathways along the bentonite-cell interface with solution percolating only through bentonite pores during permeability measurements.

Swelling pressure in permeameter cells was measured continuously by 12 force transducers FKA613 (Ahlborn) and, additionally, in the second series, by 8 force transducers 8402-6020 (burster). Upon reaching constant swelling pressure levels, fluid was injected through the inlet at the cell bottom at a pressure of 0.2 MPa using a pump and the permeability was calculated from the mass of solution percolating into collecting vessels through the outlet at the cell top (Figure 1). The dynamic viscosity of (2.084 ± 0.003) μPa·s was determined for VGH at 25 °C from nine replicate measurements.

On the 79th day of the first series of permeameter experiments, an operational malfunction of the piston pump (BESTA HD 2-200) caused an abrupt increase of the fluid injection pressure to 12.6 MPa, which persisted for about 45 min (Figure 2). In the second series, a fluid injection pressure of 0.2 MPa was prescribed, but increased initially to 0.3 MPa upon connecting the permeameter cells to the pump and then on the 86th day to 0.44 MPa (Figure 2).

Results and discussion

Swelling pressure and permeability

For different bentonites (amongst others, from Milos and Wyoming) with smectite content of at least 50 wt.%, to which no treatment other than grinding was applied prior to compaction to dry densities of 1.46—1.62 g/cm^3, swelling pressures in the range 1.2—5.4 MPa were observed upon saturation with 3 M NaCl solution [6]. For comparison, swelling pressures in the range 4.2—7.6 MPa were observed for these bentonites upon saturation with de-ionized water [6]. Swelling pressures of 2.8 MPa and 2.9—3.1 MPa were observed for FEBEX bentonite saturated with a 2.5 M NaCl solution at a dry density of 1.65 g/cm^3 [7] and for GMZ01 bentonite saturated with a 2 M NaCl solution at a dry density of 1.70 g/cm^3 [8, 9], respectively. Swelling pressures in the range 1.2—4.8 MPa observed for 11 out of 15 original bentonites in the present study upon saturation with VGH solution with a molarity of 2.6 M (Tab. 1) compare well with the previously reported values. Still, swelling pressures of 0.7—0.9 MPa for B19 and 0.3 MPa for B12 and B37 are considerably lower than those observed in the work [6] for similar dry densities. The reason for this deviation can be a deviating mode of saturation of bentonites used in the latter work with their consecutive one-week saturation by distilled water, 0.1 M, 0.3 M, 1 M and only after that by 3 M NaCl solution. Obviously, during the first 1—4 weeks of contact, a much stronger difference between ion concentrations in the initial solution of nanopores between montmorillonite crystallites and in the saturating water (saturating solution) existed in this case, as compared to the experiments of the present work, which necessarily should have led to a stronger uptake of water into these nanopores and to a higher swelling pressures. Swelling pressures of 0.0 MPa for B23 was obtained in the first series, probably, because of an unidentified defect of — possibly, a sealing ring of the load-transfer ram of — the permeameter.

*Table 1. Swelling pressures (P_s) and permeabilities (p) of original bentonites ($P_{s,i}$ and p_i) and bentonites after contact with VGH ($P_{s,r}$ and p_r) before and after fluid pressure surges of 12.6 MPa in the first and 0.3 MPa in the second*** series of permeameter experiments**

	$P_{s,i}$, MPa (before surge)	$P_{s,i}$, MPa (after surge)	p_i, m²	$P_{s,r}$, MPa*** (before surge)	$P_{s,r}$, MPa *** (after surge)	p_r, m² ***
B04	3.64 ± 0.01	2.48 ± 0.01	$8.1\cdot10^{-20}$	1.40 ± 0.01	0.48 ± 0.01	$1.9\cdot10^{-18}$
B09	1.26 ± 0.01	0.75 ± 0.01	$1.1\cdot10^{-18}$	0.13 ± 0.04**	0.21 ± 0.05**	$5.4\cdot10^{-18}$
B10	3.91 ± 0.01***	3.91 ± 0.01***	–****	0.54 ± 0.05**	0.20 ± 0.03**	$1.7\cdot10^{-18}$
B11	2.30 ± 0.01	1.99 ± 0.01	$3.9\cdot10^{-19}$	0.30 ± 0.04**	0.19 ± 0.09**	$5.4\cdot10^{-18}$
B12	0.35 ± 0.01	0.17 ± 0.01	$2.0\cdot10^{-18}$	1.09 ± 0.05**	0.68 ± 0.09**	$9.9\cdot10^{-19}$
B13	2.89 ± 0.01	1.99 ± 0.01	$6.1\cdot10^{-19}$	1.02 ± 0.01	0.72 ± 0.01	$2.7\cdot10^{-18}$
B16	1.18 ± 0.01	0.93 ± 0.01	$2.1\cdot10^{-18}$	0.19 ± 0.05**	0.37 ± 0.08**	$5.2\cdot10^{-18}$
B19	0.73 ± 0.01 0.88 ± 0.02***	0.53 ± 0.01 0.86 ± 0.02***	$3.1\cdot10^{-18}$ $1.6\cdot10^{-18}$	0.93 ± 0.01	0.72 ± 0.01	$4.3\cdot10^{-18}$
B23	0.00 ± 0.01	0.00 ± 0.02	$3.0\cdot10^{-17}$	0.48 ± 0.05**	0.51 ± 0.09**	$2.3\cdot10^{-18}$
B31	4.72 ± 0.01	3.94 ± 0.01	$5.0\cdot10^{-19}$	0.78 ± 0.02	0.52 ± 0.02	$2.6\cdot10^{-18}$
B36	2.67 ± 0.01	2.13 ± 0.01	$9.7\cdot10^{-18}$	0.69 ± 0.07** 0.69 ± 0.01	0.91 ± 0.09**	$1.0\cdot10^{-17}$ $1.4\cdot10^{-17}$
B37	0.31 ± 0.01	0.31 ± 0.01	$2.0\cdot10^{-17}$	1.39 ± 0.04	0.89 ± 0.01	$4.1\cdot10^{-19}$
B38	1.60 ± 0.01***	1.63 ± 0.01***	$1.9\cdot10^{-18}$	0.55 ± 0.01	0.56 ± 0.01	$1.8\cdot10^{-17}$
B49	4.28 ± 0.06***	3.25 ± 0.01***	$1.0\cdot10^{-18}$	1.98 ± 0.05**	1.73 ± 0.08**	$2.4\cdot10^{-18}$
SD80	4.85 ± 0.01***	4.98 ± 0.02***	$6.9\cdot10^{-20}$	1.34 ± 0.01 2.21 ± 0.01	1.28 ± 0.01	$6.9\cdot10^{-19}$ $2.5\cdot10^{-19}$

*second values in in the cells of the table for B19, B36, and SD80 represent results of replicate measurements
**values obtained with force transducers from burster
***values obtained n the second& series of experiments
****no value could be obtained because of absent percolation through bentonite pellet

Laboratory and *in situ* permeabilities of argillaceous rocks were found to vary in the range 10^{-23}—10^{-17} m² [10, 11]. Permeabilities measured for original bentonites and bentonites after one-year contact with VGH in the present study are within this range as well (Tab. 1). Original B04 and SD80 from Milos (Greece) at dry densities of 1.52—1.53 g/cm³ show the lowest average permeability of about $6.9\cdot10^{-20}$ m², which is comparable to a permeability of $(9.2—9.4)\cdot10^{-20}$ m² (calculated from the reported hydraulic conductivities) measured for a 2 M NaCl solution and GMZ01 bentonite at a higher dry density of 1.70 g/cm³ [8, 9]. According to [2] the integral permeability of bentonite-based barriers in repository concepts in German clay formations should not exceed $2\cdot10^{-17}$ m². It can be seen from the present data that at the applied dry densities in the range 1.47—1.59 g/cm³ all original bentonites, except for B23, and all bentonites, which contacted for one year with VGH, would comply with this requirement, albeit the average permeabilities of $1.8\cdot10^{-17}$ m² for original B37 and B38 after one-year contact with VGH lie very close to this limit. A comparison for original bentonites and bentonites after one-year contact with VGH shows further that only for B12, B23, and B37, a significant increase of swelling pressure (after surge) and a decrease of permeability occurred upon the contact with VGH (Table 1). Establishing reasons for this deviating behaviour would require microstructural analyses and was beyond the scope of the present study.

Effect of microstructural re-organization

Bentonite swelling behaviour observed in many studies upon saturation with solutions of low salinity (as discussed, e. g., by [12]) is characterized by a rapid initial increase (e. g., within 10 hours for GMZ01 bentonite [8]), followed by an intermediate decrease of the swelling pressure, and a second increase (e. g., after about 30—40 hours for GMZ01 bentonite [8, 13]) to a final steady-state value. This "double-peak" pattern of swelling pressure evolution is explained by (i) a rapid swelling of aggregates (the first peak), followed by (ii) a deformation and, upon a sufficient hydration, a partial decomposition of aggregates with an accompanying collapse of the pores between the aggregates (depression after the first peak), and (iii) the final swelling of the

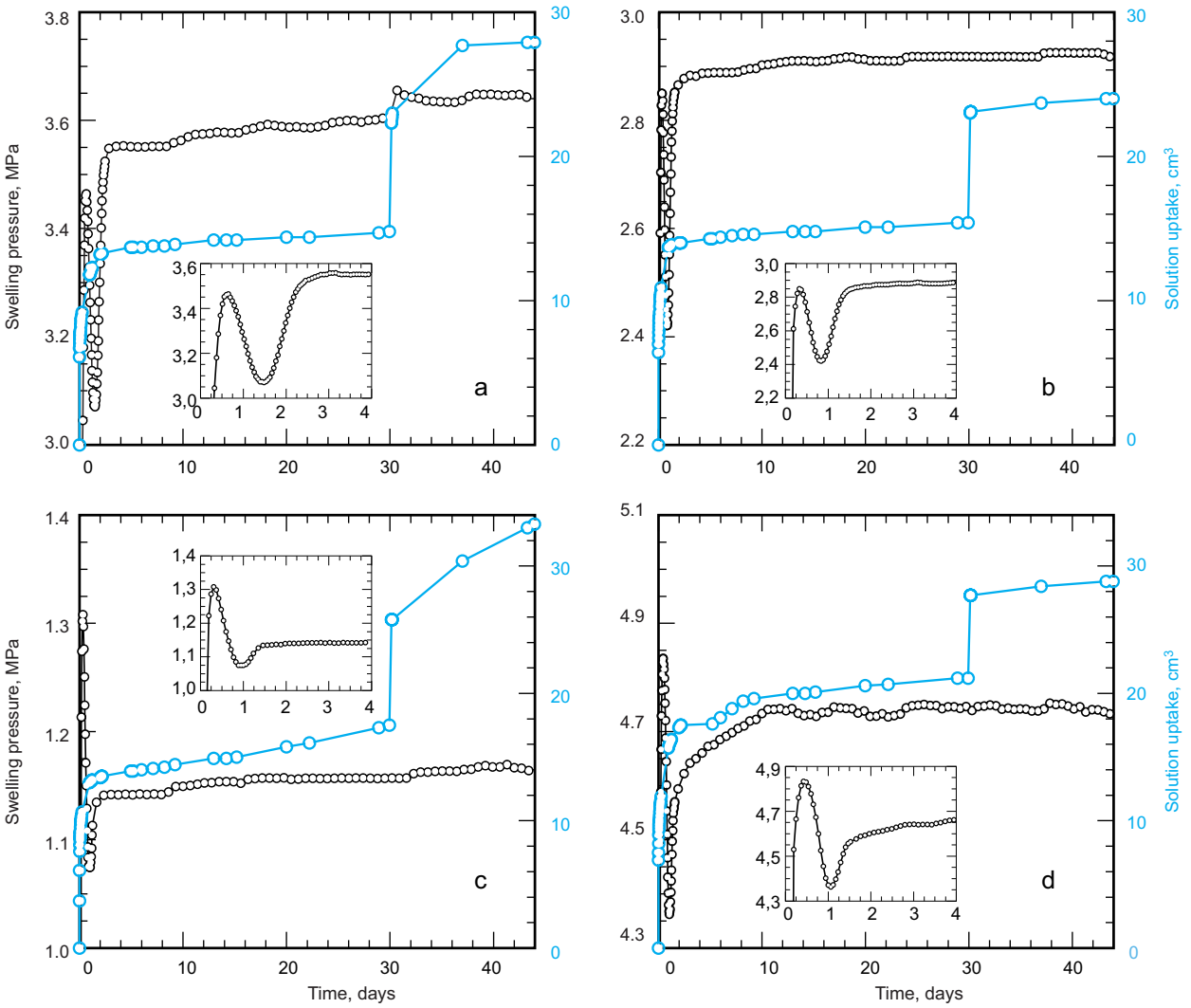

Figure 3. Swelling pressure and solution uptake for original B04 (a), B13 (b), B16 (c), and B31 (d) at respective dry densities of 1.52, 1.52, 1.54, and 1.57 g/cm³ upon saturation with VGH (supplied by burettes connected to inlets at cell bottoms for 30 days and at cell tops afterwards). Insets show close-ups for the first four days of saturation

then re-organized and partially smaller aggregates (the second peak) [12]. At dissolved salt concentrations above ~ 0.5 M, only the first peak was observed for GMZ01 bentonite [8].

Although VGH is characterized by a considerably higher dissolved salt concentration of 2.6 M, the double-peak pattern of swelling pressure evolution was still observed for original B04, B13, B16, and B31 (Figure 3). This observation suggests that the occurrence of the double-peak pattern at higher salinities of saturating solutions may depend on bentonite type. Swelling pressure evolution observed here features a higher second peak for original bentonites B04 and B13, similarly to previous observations (see [8, 12, 13] and references therein), but, differently from those works, a lower second peak for original bentonites B16 and B31 (Figure 3). A reason for this observation might be the high salinity of saturating VGH.

It can be further seen from Figure 3 that although compacted bentonite absorbed 8 up to 16 ml solution from burettes connected to inlets at cell tops, which makes 50 up to nearly 100 % of the volume absorbed previously through the inlets at cell bottoms, no correspondent increase of swelling pressure occurred, except for a small one for B04. This may suggest that nanopores between montmorillonite crystallites and intra-aggregate micropores, responsible for the swelling pressure evolution as discussed before, at the top side of bentonite pellets were already saturated with water, except, probably, for a small portion of such pores in B04. Accordingly, the solution arriving from the cell tops would only saturate the inter-aggregate micropores hardly contributing to the macroscopic swelling pressure.

It is noticeable that differently from the swelling behaviour in the first series, characterised by a rapid initial increase of swelling pressure (Figure 3,

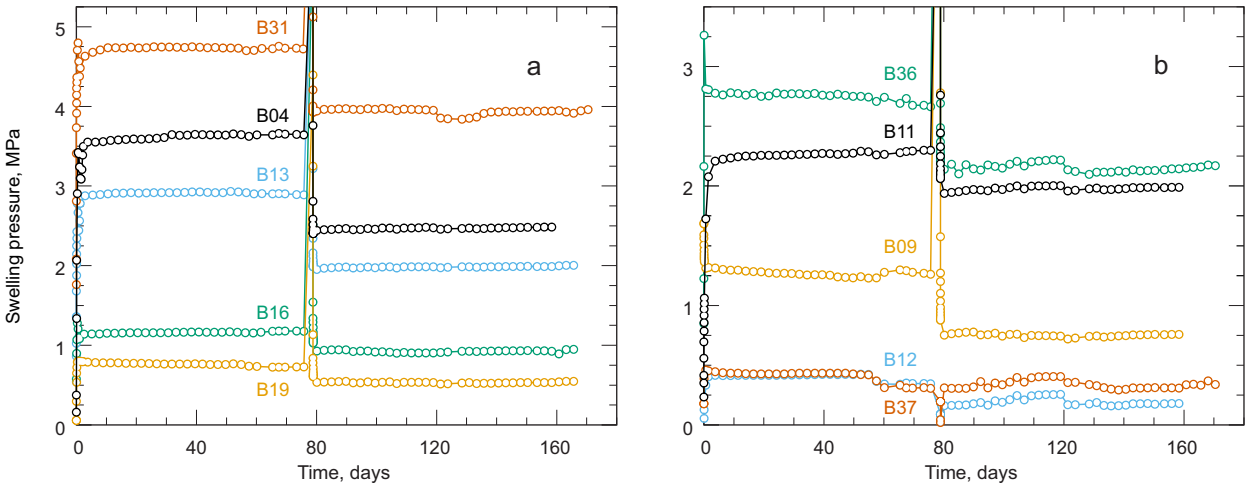

Figure 4. Swelling pressure evolution for original bentonites B04, B13, B16, B19, and B31 (a) and B09, B11, B12, B36, and B37 (b) upon saturation with VGH in the first series. VGH was supplied by burettes for 44 to 57 days and by a pump afterwards

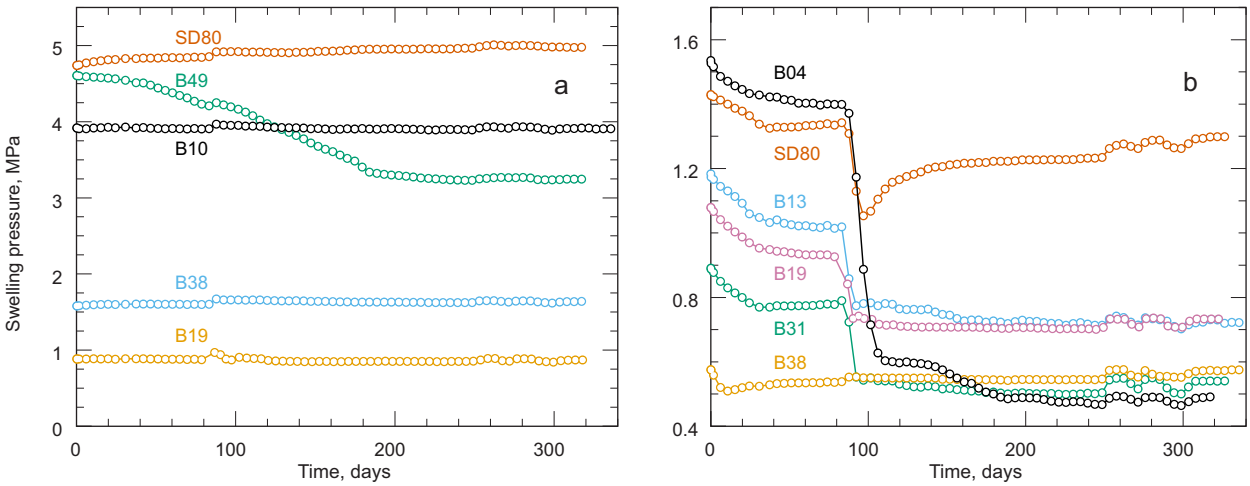

Figure 5. Swelling pressure evolution for original bentonites B10, B19, B38, B49, and SD80 (a) and bentonites B04, B13, B19, B31, B38, and SD80 after one-year contact with VGH (b) upon saturation with VGH in the second series. VGH was supplied by burettes for 75 days and by a pump starting from the 85th day

Figure 4), no such increase and, correspondingly, no double-peak pattern were observed in the second series for both, original bentonites and bentonites after one-year contact with VGH (Figure 5). A probable reason for this observation may be the triple loading/unloading of compacted bentonites in advance of the contact with VGH applied in the second series. Comparison of swelling behaviours observed for original B19 in the first and the second series (Figure 4a, Figure 5b) support this suggestion, as the triple loading/unloading was the only major difference in the preparation of the two tests with this bentonite.

A preliminary desiccation of bentonites at high suction pressures was found to cause a destruction of large aggregates and microstructural re-organization accompanied by an increase of swelling pressure [14] in a process apparently very similar or identical to that occurring during hydration as discussed above. An assumption that the energy supplied during the loading/unloading suffice for triggering a destruction of large aggregates and microstructural re-organization might then explain the lacking double-peak pattern of swelling pressure evolution and the lacking rapid increase of swelling pressure in the second series. The observed decreases of stress necessary to compact bentonites B10, B38, and SD80 to the prescribed density of 1.6 g/cm^3 during the consecutive loadings (Figure 6) indicate occurring of microstructural adjustments during the intermediate unloadings which may support this argumentation. Yet, such stress decreases do not occur for B49 (Figure 6), which might be putatively attributed to some re-organisational reluctance pertinent to its microstructure. Indeed, differently from the other original bentonites, B49

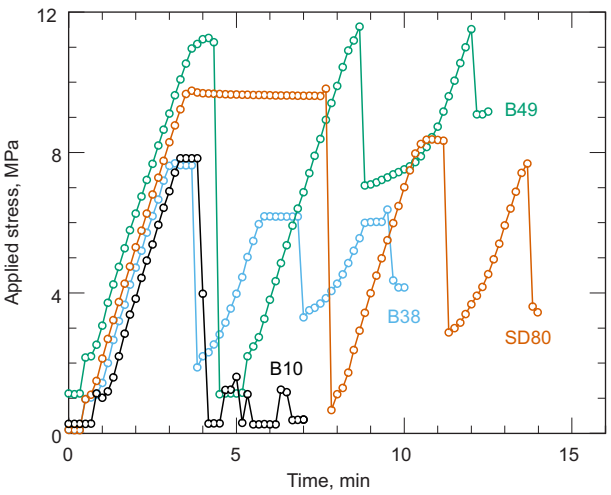

Figure 6. Stress applied during a triple consecutive compaction of B10, B38, B49, and SD80 to the density of 1.6 g/cm³ and intermediate unloadings

did not show a rapid microstructure re-organization upon saturation with VGH but rather a very slow one over a period of about 180 days (Figure 5a).

Influence of fluid pressure surges on swelling pressure and permeability

In the first series, pressure of solution supplied to the bottoms of permeameter cells surged from 0.2 to 12.6 MPa on the 78th day and remained at this level for about 45 min (Figure 2), which caused considerable decreases of swelling pressure by 13 up to 51 % for 9 of 11 bentonites at the end of this time interval (Figure 4, Table 1). Upon this fluid pressure surge, force transducers in the cell tops registered an additional load of 6.1 MPa for B19, 9.8—10.2 MPa for B04, B11, B13, and B16, 10.9 MPa for B09, 11.7 MPa for B36, and 12.2 MPa for B31 (no records during the pressure surge were delivered by force transducers in tests with B12 and B37 presumably because of overload).

The fact that the fluid pressure of 12.6 MPa remained nearly unchanged during the whole duration of pressure surge (~45 min), after which the pump restored the prescribed fluid injection pressure of 0.2 MPa (Figure 2), evidences that no hydraulic fracture formed in the bentonite pellets. The accompanying additional loads recorded by force transducers can be then inferred to result from the increased mechanical stress on the pellets, which was passed down to the force transducers by the mineral skeleton of samples. The different mechanical loads passed down to the force transducers by different bentonites can be accordingly explained by different extent of microstructural deformations in bentonites.

Furthermore, no considerable increase of volume of solution infiltrating through pellets, which would also evidence hydraulic fracturing inside pellets or at their interface with cell walls, occurred for studied bentonites (Figure 7a). Although permeability increased for B16 and B36 by a factor of 1.8 and 4.1, respectively, upon the pressure surge, it remained at a low level of $(1.3—6.9)\cdot10^{-18}$ m², which evidences that no fracture flow occurred through these bentonites. The first solution percolation through bentonites B04, B11—B13, and B31 occurred on the next day after the pressure surge (Figure 7b), which indicates a cause-effect relationship between these events. However, their permeabilities calculated assuming that percolation started upon the pressure surge were in the range $4.7\cdot10^{-19}—5.2\cdot10^{-18}$ m² (Figure 7b), which evidences that no fracture flow occurred through these bentonites either. Eight days later, permeabilities of these bentonites decreased down to $1.0\cdot10^{-19}$ to $2.0\cdot10^{-18}$ m² (Figure 7b).

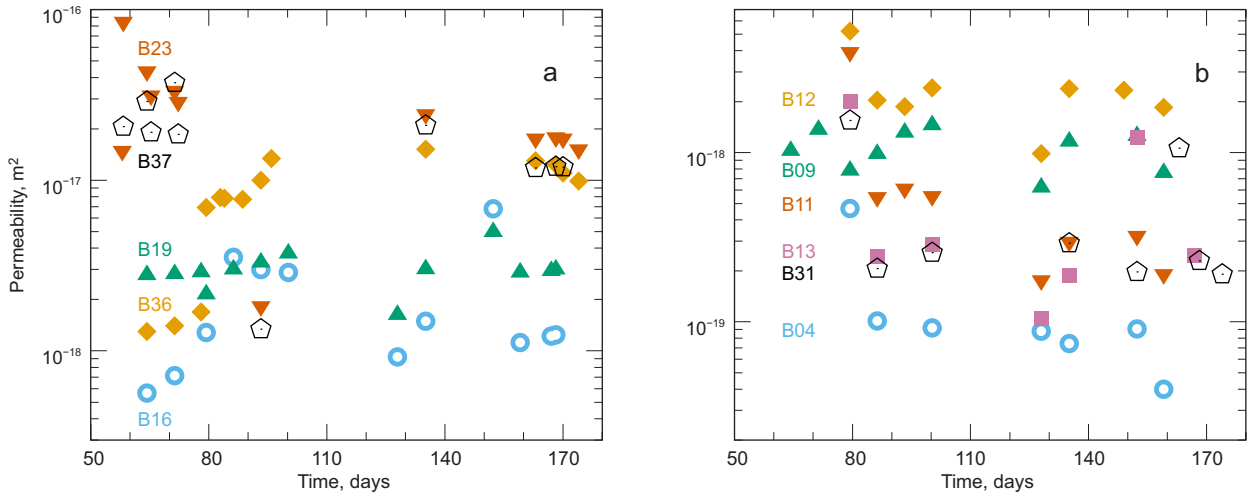

Figure 7. Permeability of original bentonites for VGH (m²) in the first series

In experiments with bentonite Kunigel V1 compacted to a dry density of 1.6 g/cm^3, the onset of hydraulic fracturing was observed within several minutes upon increasing the fluid injection pressure to threshold values of 3.2 up to 4.7 MPa, whereas for its 70:30 mixture with sand even broader variation of threshold values from 2 to 8 MPa was measured [3]. The question then arises, why bentonites studied here are characterized by a much higher strength for hydraulic fracturing of at least 12.6 MPa than Kunigel V1. Swelling pressure, which was argued to strongly influence the breakdown pressure [3], varies broadly for studied bentonites (Table 1) below and above the value of 1.8 MPa measured for Kunigel V1 [3] and, hence, cannot be a reason for this difference. Similarly, the water content, increase of which was argued to decrease the strength for hydraulic fracturing [3], cannot be a reason for this difference as well, as at the time of pressure surge studied bentonites were saturated with water and its content (around 25 %) was much higher than that of 12.5 % for Kunigel V1 [3]. It ought to be then concluded that the reason for the difference can be the different experimental setup used in [3], which featured a tube with a diameter of 2 mm for a point-wise injection of water into an unsaturated bentonite compacted around the tube. Such a setup appear to be not transferable to the setup in the present study with the solution being injected over a surface with an area of 19.6 cm^2 from outside the compacted bentonite, which is thought to closer resemble the expected situation in a repository.

In the second series, the fluid pressure surged upon the switching on the pump from 0 to 0.28 MPa and then to 0.44 MPa with the consequence that swelling pressures decreased within about two (B13) to 20 (B04) days in a first, relatively steep step and within further up to 80 days in a second, more gradual step by up to 66% for 9 of 15 bentonites after one-year contact with VGH (Figure 5b, Table 1). Tests with B19 (Figure 5) illustrate that one-year contact with VGH at 25 °C can apparently cause some relevant changes of its microstructure, as its swelling pressure decreased by 23 % while that of original B19 did not show any significant change upon the same fluid pressure surge. A mode of microstructural modification obviously deviating from that for the other studied bentonites was observed for SD80 after one-year contact with VGH, swelling pressure of which decreased by 0.37 MPa within 10 days after the fluid pressure surge, but increased steadily within following 230 days and nearly reached the original value at the end of the test (Figure 5b).

Presented data allow to suggest that the decreases of swelling pressure upon fluid pressure surges must originate from a process leading depending on bentonite type to different modes of microstructural re-organisation. An additional compaction of bentonite pellets during the pressure surge, which would lead to a decreased pellet height and to an accordingly decreased force exerted by pellet on the force transducers of the permeameter cell, can be discarded as a possible reason considering that in the second series this process proceeds rather slowly, on the scale of several days to several weeks (Figure 5b). This process may be a reverse one to that of destruction of large aggregates discussed in the preceding section and lead to a formation of larger aggregates and larger pores in bentonite and thus to lower macroscopic swelling pressures.

Concluding remarks

No hydraulic fracturing occurred in compacted original bentonites as a result of the fluid pressure surge of 12.6 MPa, which however led to a twofold decrease of their swelling pressures, presumably, as a result of a plastic deformation in compacted bentonites, which partially absorbed the energy input of the pressure surge. Similar decreases of swelling pressures occurred for bentonites compacted after their one-year contact with VGH at 25 °C upon a much smaller fluid pressure increase of 0.3 MPa. It remains to be understood which microstructural changes are responsible for these macroscopic observations. Provided independent confirmation of the reported observations and that occurrence of fluid pressure surges either as a result of gas accumulation and release or other processes in repository can represent a possible scenario of its evolution, gaining such understanding would be of particular importance for design of bentonite-based barriers and their performance assessments. It may be also reasonable to prove whether the effect of fluid pressure surges on compacted bentonites can be considered as a conservative limit for the effect of the expected gradual increase of fluid pressure in the course of restoration of hydraulic conditions in the host formation upon the repository closure.

Acknowledgement

Funding of the study by the Federal Ministry of Economic Affairs and Energy (BMWi), represented by the Project Management Agency Karlsruhe (PTKA-WTE), contract no. 02E11344A, is gratefully acknowledged. Dr. Stephan Kaufhold (BGR, Hannover) is gratefully acknowledged for providing bentonites. The experimental results were obtained owing to a skilful lab work of Michael Kröhn (swelling pressure and permeability experiments)

and Veronika Prause (preparation of bentonites and solution, water contents) of the geoscientific laboratory of the GRS. Discussions with Dr. Chun-Liang Zhang (GRS) on experimental design and results are gratefully acknowledged.

References

1. Jobmann M., Bebiolka A., Burlaka V., Herold P., Jahn S., Lommerzheim A., Maßmann J., Meleshyn A., Mrugalla S., Reinhold K., Rübel A., Stark L., Ziefle G. Safety assessment methodology for a German high-level waste repository in clay formations. *Journal of Rock Mechanics and Geotechnical Engineering*. 2017. Vol. 9. Pp. 856—876.
2. Jobmann M., Bebiolka A., Jahn S., Lommerzheim A., Maßmann J., Meleshyn A., Mrugalla S., Reinhold K., Rübel A., Stark L. Ziefle G. *Sicherheits- und Nachweismethodik für ein Endlager im Tongestein in Deutschland — Synthesebericht*. Ber.-Nr. TEC-13-2016-AB, DBE TECHNOLOGY, BGR, GRS, Peine, Hannover, Braunschweig, 2017, 137 p.
3. Kobayashi A., Yamamoto K., Momoki S. Characteristics of strength for hydraulic fracturing of buffer material. *Soils and Foundations*. 2008. Vol. 48. Pp. 467—477.
4. Chen Y. G., Jia L. Y., Ye W. M., Chen B., Cui Y. J. Advances in experimental investigation on hydraulic fracturing behavior of bentonite-based materials used for HLW disposal. *Environmental Earth Sciences*. 2016. Vol. 75. Pp. 1—14.
5. Kaufhold S., Hein M., Dohrmann R., Ufer K. Quantification of the mineralogical composition of clays using FTIR spectroscopy. *Vibrational Spectroscopy*. 2012. Vol. 59. Pp. 29—39.
6. Karnland O., Olsson S., Nilsson U. *Mineralogy and sealing properties of various bentonites and smectite-rich clay materials*. Report TR-06-30, SKB, Stockholm, 2006, 70 p.
7. Lloret A., Villar M. V. Advances on the knowledge of the thermo-hydro-mechanical behaviour of heavily compacted "FEBEX" bentonite. *Physics and Chemistry of the Earth*. Parts A/B/C. 2007. Vol. 32. Pp. 701—715.
8. Zhu C. M., Ye W. M., Chen Y. G., Chen B., Cui Y. J. Influence of salt solutions on the swelling pressure and hydraulic conductivity of compacted GMZ01 bentonite. *Engineering Geology*. 2013. Vol. 166. Pp. 74—80.
9. Chen Y. G., Zhu C. M., Ye W. M., Cui Y. J., Wang Q. Swelling pressure and hydraulic conductivity of compacted GMZ01 bentonite under salinization–desalinization cycle conditions. *Applied Clay Science*. 2015. Vol. 114. Pp. 454—460.
10. Brace W. F. Permeability of crystalline and argillaceous rocks. *International Journal of Rock Mechanics and Mining Sciences & Geomechanics Abstracts*. 1980. Vol. 17. Pp. 241-251.
11. Neuzil C. E. How permeable are clays and shales? *Water Resources Research*. 1994. Vol. 30. Pp. 145—150.
12. Yigzaw Z. G., Cuisinier O., Massat L., & Masrouri F. Role of different suction components on swelling behavior of compacted bentonites. *Applied Clay Science*. 2016. Vol. 120. Pp. 81—90.
13. Ye W. M., Wan M., Chen B., Chen Y. G., Cui Y. J., Wang J. Temperature effects on the swelling pressure and saturated hydraulic conductivity of the compacted GMZ01 bentonite. *Environmental Earth Sciences*. 2013. Vol. 68. Pp. 281—288.
14. Lang L. Z., Baille W., Tripathy S., Schanz T. Experimental study on the influence of preliminary desiccation on the swelling pressure and hydraulic conductivity of compacted bentonite. *Clay Minerals*. 2018. Vol. 53. Pp. 733—744.

Information about the author

Meleshyn Artur Yurievich, Dr. rer. nat., researcher, Gesellschaft für Anlagen- und Reaktorsicherheit (GRS) gGmbH (4, Theodor-Heuss-Straße, Braunschweig, D-38122, Germany), e-mail: artur.meleshyn@grs.de.

Bibliographic description

Meleshyn A. Yu. Swelling Behaviour and Permeability of Compacted Bentonites at High Salinity as Influenced by Fluid Pressure Changes. *Radioactive Waste,* 2020, no. 2 (11), pp. 109—119. (In Russian). DOI: 10.25283/2587-9707-2020-2-109-119.